Fast Ignitron Trigger Circuit Using Insulated Gate Bipolar Transistors

Vernon H. Chaplin and Paul M. Bellan

***Abstract*— This paper describes a low cost, easy-to-implement circuit for triggering ignitrons in plasma physics experiments and other pulsed power applications. Using insulated gate bipolar transistors (IGBTs) for rapid switching, the circuit delivers > 200 A peak current from a 0.1-μF capacitor to the ignitron trigger pin with a rise time of ∼0.6 μs. The trigger circuit is isolated from the ignitron by a pulse transformer. Details of the circuit design and practical considerations for working with IGBTs are discussed. Sources of inductance in the system are identified, and leakage inductance associated with the pulse transformer is shown to be the primary factor limiting the pulse rise time.**

***Index Terms*— IGBT, ignitron, pulse transformer, pulsed power.**

I. Introduction

IGNITRONS, plasma-based rectifiers containing mercury, are used to switch large currents (up to 100 kA for Size A ignitrons) on μs–ms timescales in many pulsed plasma experiments [1]–[4]. Triggering an ignitron into conduction requires the application of a high voltage (1.5–3 kV), high current (100–250 A) pulse to the ignitor, a semiconducting rod which extends into the mercury pool that forms the ignitron's cathode. Variance in turn-on time (jitter) will be minimized and ignitron lifetime prolonged if a high energy trigger pulse with peak current near the rated maximum is used [5].

This paper describes a simple ignitron driver circuit for achieving fast, reliable triggering with minimal jitter. Ignitron triggering is typically achieved with a capacitor discharge circuit; in the past, these circuits have often used krytrons [6]–[8] or thyristors/silicon-controlled rectifiers (SCRs) [9]–[11] as switches. However, SCRs are not fast enough for some plasma experiments, (turn-on times generally limited to a few μs), and krytrons are no longer manufactured and are difficult to acquire due to legal restrictions. In recent years, insulated gate bipolar transistors (IGBTs) have been developed that combine high voltage and current handling capability with fast switching times, providing a superior alternative. The IXYS IXEL40N400 IGBT [12], used in this paper, is rated for a collector-emitter voltage of 4 kV and a peak current of 240 A, with a < 3 cm^3 package volume. The circuit uses two of these IGBTs in parallel to deliver 230 A peak to the ignitron trigger, with a rise time of ~ 0.6 μs (see Fig. 1). The current rise time is largely limited by the load impedance (consisting of the ignitron, trigger transformer, and connecting wires); with an 8-Ω resistive load, the circuit can achieve $dI/dt > 1.2$ kA/μs. A detailed analysis of the sources of inductance in the load will be presented in Section V.

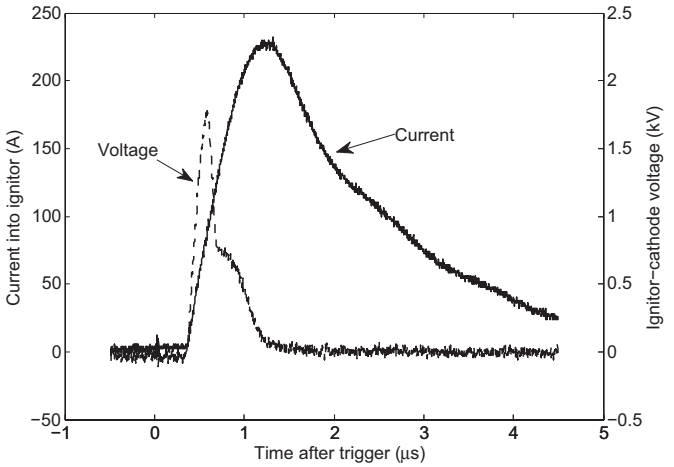

Fig. 1. Voltage and current at the ignitron ignitor during a trigger pulse from the IGBT-based driver circuit. Initially, the ignitron acts approximately like a 22-Ω resistor, with $V_{\text{ignitor}} \approx 22 \times I_{\text{ignitor}}$. At $t \approx .58$ μs, the ignitor-to-cathode impedance begins to change, presumably due to mercury plasma breakdown in the ignitron, and from this point forward the voltage is no longer directly proportional to the current. Voltage was measured with a Tektronix 6015A high voltage probe and current was measured with an Ion Physics Model CM-1-L current monitor.

II. Circuit Overview

A partial circuit diagram is shown in Fig. 2. A 0.1-μF capacitor, charged to 3 kV by an EMCO G30 proportional power supply, is discharged through the IGBTs and a 1:2 pulse transformer (wound with Style 3239 #20 AWG 30 kVDC wire on a Ferroxcube U93/76/30-3C81+I93/28/30-3C81 U-core+I-core ferrite pair) with the secondary winding connected between the ignitron's ignitor and cathode. A 4.2-Ω resistor in series with the ignitor limits the peak current into the ignitron. Although a step-up transformer is used, the voltage on the ignitor never exceeds 2 kV due to voltage divider effects caused by impedances between the circuit board and the ignitor (see Figs. 1 and 6 and the discussion in Section V). The trigger signal to turn on the IGBTs is provided by a 1-μF capacitor charged to 24 V and switched by a

Manuscript received July 15, 2012; revised December 21, 2012; accepted February 7, 2013. Date of current version April 6, 2013. This work was supported by U.S. DOE, the National Science Foundation, and AFOSR.

The authors are with the Applied Physics Department, California Institute of Technology, Pasadena, CA 91125 USA (e-mail: vchaplin@caltech.edu; pbellan@caltech.edu).

Color versions of one or more of the figures in this paper are available online at http://ieeexplore.ieee.org.

Digital Object Identifier 10.1109/TPS.2013.2249113

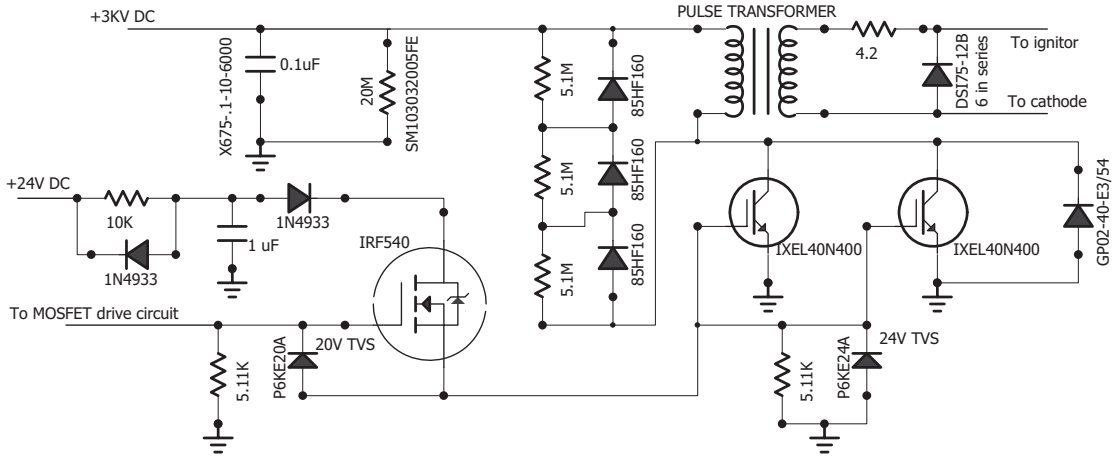

Fig. 2. Partial circuit diagram for the ignitron driver.

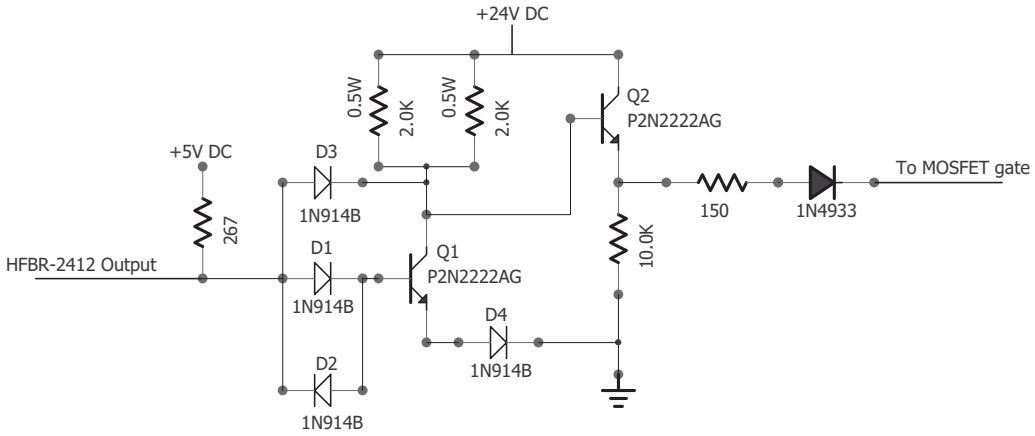

Fig. 3. Circuit for triggering the MOSFET switch.

MOSFET. Switching is initiated by an optical trigger delivered to an Avago HFBR-2412 fiber optic receiver (see Fig. 3).

Three 85HF160 diodes in series are connected across the transformer primary to protect the IGBTs from switching transients and maintain $V_{\mathrm{CE}} \geq 0$. Transient voltage suppression (TVS) diodes between the IGBT gate and emitter and between the MOSFET gate and source protect against overvoltages that could be caused by inductive pickup. Protective diodes (six DSI75–12B in series) are also installed on the secondary side of the pulse transformer to prevent the ignitor-cathode voltage from becoming negative. The circuit operates off a single 24 V, 10-W DC power supply, with voltage regulator chips on the board providing 5- and 12-V DC voltages.

III. Details of IGBT Drive Circuit

In order to turn on the IXEL40N400 IGBT, approximately 270 nC of charge must be deposited on the gate. The gate-emitter voltage required for turn-on varies with collector current: at $I_C = 20$ A, $V_{\mathrm{GE}} = 12$ V will suffice, while at $I_C = 80$ A, $V_{\mathrm{GE}} \geq 15$ V is required [12]. In our circuit, the gate is charged by discharging a 1-μF capacitor through an IRF540 MOSFET. Note that for many similar applications, an inexpensive commercial IGBT gate driver IC, such as Diodes Incorporated model ZXGD3005E6, could be used in lieu of the custom driver circuit presented here.

MOSFETs have similar turn-on behavior to IGBTs, but with lower drive voltage and charge requirements. The switching circuit that triggers the MOSFET is shown in Fig. 3. An optical pulse causes the voltage on the open collector output of the HFBR-2412 receiver to drop to ~ 0.5 V, turning off the NPN transistor $Q1$ and causing the voltage on its collector to rise to nearly 24 V. An emitter follower implemented with the NPN transistor $Q2$ provides current gain for fast charging of the MOSFET gate. Diodes $D1$ through $D4$ form a modified Baker clamp [13], which maintains the condition $V_C - V_E \geq \Delta V_D$ on the voltages on $Q1$'s terminals (where ΔV_D is the diodes' on-state voltage drop), preventing the transistor from saturating and allowing for rapid turn-off.

IV. Circuit Layout

Proper circuit layout is critical for achieving fast switching times with IGBTs [14]. Any inductance between the IGBT's emitter and the circuit ground will cause the emitter voltage to rise by $L dI_C/dt$ as the discharge current ramps up, lowering V_{GE} and slowing IGBT turn-on. With $dI_C/dt = 500$ A/μs, L need only be 10 nH to depress V_{GE} by 5 V. IGBT packages have some internal inductance, but the negative

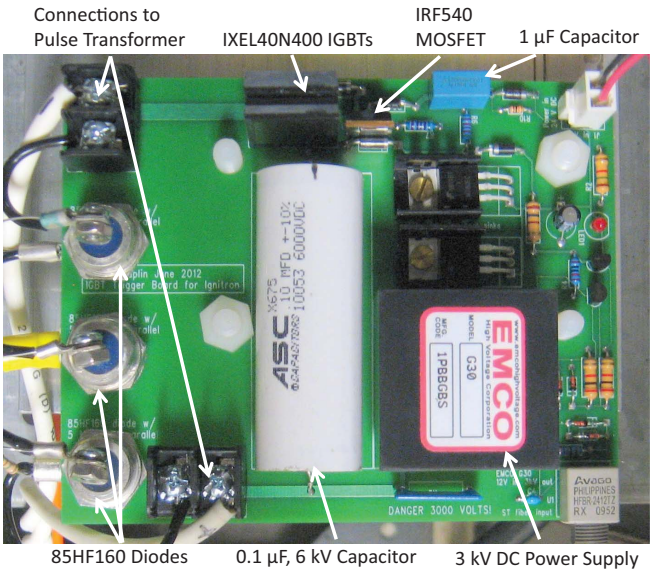

Fig. 4. Photo of finished ignitron trigger board. The board dimensions are 4 inches by 5 inches.

effects can be minimized by connecting the IGBT emitter as close to the ground side of the discharge capacitor as possible. The LdI_G/dt voltage drop along the wire connecting the IGBT drive circuit to the gate is also detrimental to fast switching. Taking these considerations into account, we mounted the IGBTs, MOSFET, and 0.1- and 1-μF capacitors as close together as possible on the circuit board, with wide copper tracks connecting the components and the bulk of the underside of the board serving as a ground plane (see the photo in Fig. 4).

V. Effect of Pulse Transformer Coupling on Rise Time

Comparatively little care was taken to optimize the layout of the wires between the trigger board, pulse transformer, and ignitron, as nonideal behavior of the pulse transformer itself was found to be the primary factor limiting the pulse rise time. Since the primary and secondary windings in a real transformer cannot occupy exactly the same position in space, there will be some deviation from the ideal transformer condition in which identical magnetic flux links the primary and secondary. This stray flux leads to an effective inductance in series with the primary or secondary—this is known as the "leakage inductance" of the transformer.

To see how leakage inductance arises from nonideal coupling between the windings, let L_1 be the primary inductance, L_2 be the secondary inductance, and M be the mutual inductance of the windings and consider a circuit with some additional inductance L_p in series with the primary and inductance L_s and resistance R_s in series with the secondary. If a voltage $V_{\text{in}}(t)$ is applied to the primary, the currents through the windings will be related by

$$L_1\dot{I}_1 + M\dot{I}_2 = V_{\text{in}}(t) - L_p\dot{I}_1 \tag{1}$$

$$M\dot{I}_1 + L_2\dot{I}_2 = -L_s\dot{I}_2 - R_sI_2. \tag{2}$$

Eliminating $\dot{I}_1$ to solve for $\dot{I}_2$ in terms of $V_{\text{in}}(t)$ and I_2:

$$\dot{I}_2 = \frac{-\left(L_1+L_p\right)R_sI_2 - MV_{\text{in}}(t)}{\left(L_1+L_p\right)\left(L_2+L_s\right) - M^2}. \tag{3}$$

Define the transformer coupling coefficient $\kappa \equiv M/\sqrt{L_1L_2}$, so that $\kappa = 1$ for an ideal transformer and $\kappa < 1$ for a real transformer. Substituting in for M, and assuming $L_1, L_2 \gg L_p, L_s$ (since the transformer is wound on a ferrite, which amplifies the flux through the primary and secondary), the previous equation becomes

$$\dot{I}_2 = \frac{-L_1R_sI_2 - \kappa\sqrt{L_1L_2}V_{\text{in}}(t)}{L_1L_2\left(1-\kappa^2\right) + L_1L_s + L_2L_p}. \tag{4}$$

Consider the response of the circuit to a step function voltage input at $t = 0$. In this case, solving the differential equation for the current through the secondary yields

$$I_2(t) = -V_{\text{in}}\frac{\kappa}{R_s}\sqrt{\frac{L_2}{L_1}}\left(1-\exp\left(-\frac{t}{\tau_r}\right)\right) \tag{5}$$

$$\tau_r \equiv \frac{1}{R_s}\frac{L_2}{L_1}\left(L_1\left(1-\kappa^2\right) + \frac{L_1}{L_2}L_s + L_p\right). \tag{6}$$

This result shows that for the purpose of determining the rise time τ_r, setting $\kappa \neq 1$ is equivalent to adding an inductance $L_1(1-\kappa^2)$ in series with the primary, or $L_2(1-\kappa^2)$ in series with the secondary. Because of the dependence on κ^2 and the fact that $L_1, L_2 \gg L_p, L_s$, a small deviation from perfect coupling will have a large effect on the rise time.

For the pulse transformer utilized in this paper, we used a B&K Precision Model 885 LCR/ESR Meter to measure $L_1 = 121.6\ \mu H$, $L_2 = 485.3\ \mu H$, and $M = 241.7\ \mu H$ (mutual inductance can be determined by measuring the inductance of the primary and secondary connected in series), so $\kappa = M/\sqrt{L_1L_2} \approx 0.995$. A more accurate measurement of κ may be made by comparing the voltage waveforms across the primary and secondary during a pulse from the ignitron trigger circuit. These waveforms are shown in Fig. 5. Although the transformer turns ratio is 1:2, the secondary voltage is not equal to twice the primary voltage since $\kappa < 1$. A good fit to the data is obtained with a leakage inductance value of 1.5 μH in series with the primary (nearly perfect agreement between the waveforms can be obtained if the measured winding resistances are also taken into account). Since the leakage inductance in series with the primary is $L_{\text{leakage}} = L_1(1-\kappa^2)$, this implies $\kappa = \sqrt{1 - L_{\text{leakage}}/L_1} \approx 0.994$.

The inductance contributed by the wiring between the circuit board, pulse transformer, and ignitron can also be measured by identifying the LdI/dt voltage drops in the circuit. Voltage waveforms at four locations are shown in Fig. 6. The voltage drop between the circuit board and the transformer primary is due to the inductance of the loops formed by the tracks on the board and the connecting wires (partially visible in Fig. 4). A good fit to the data is obtained by assuming a value $L_p = 780$ nH. Similarly, the voltage drop between the transformer secondary and the ignitor is due to the inductance of the connecting wires and also the IR voltage drop across the 4.2-Ω resistor. Setting $L_s = 900$ nH gives an

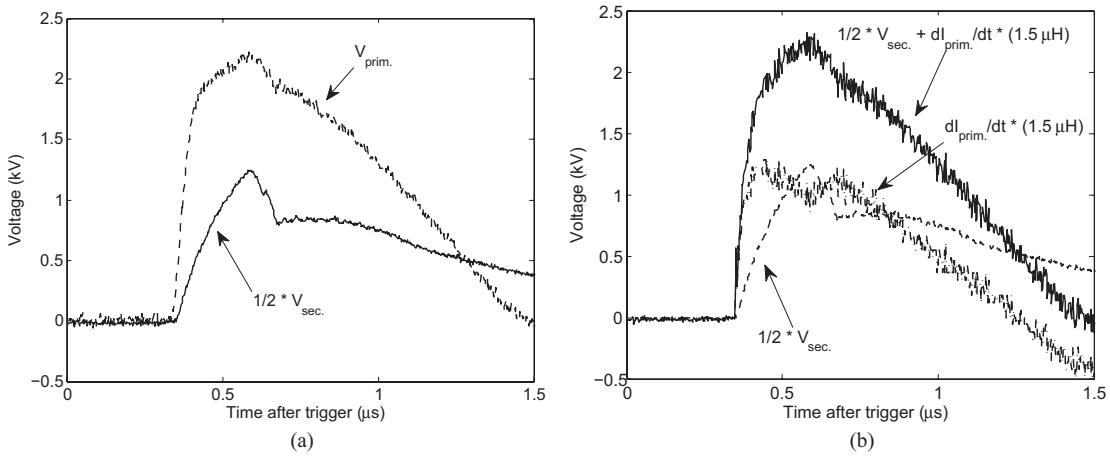

Fig. 5. Voltage across the pulse transformer primary and secondary windings during the first 1.5 μs of a pulse. If the transformer were ideal, the secondary voltage $V_{\text{sec.}}$ would be exactly twice the primary voltage $V_{\text{prim.}}$. However, the (a) actual secondary voltage is lower than this due to imperfect coupling of flux between the primary and secondary. If a 1.5-μH leakage inductance is assumed to be present in series with the primary, the (b) associated LdI/dt voltage drop accounts for the discrepancy between the $V_{\text{prim.}}$ and $V_{\text{sec.}}$ waveforms.

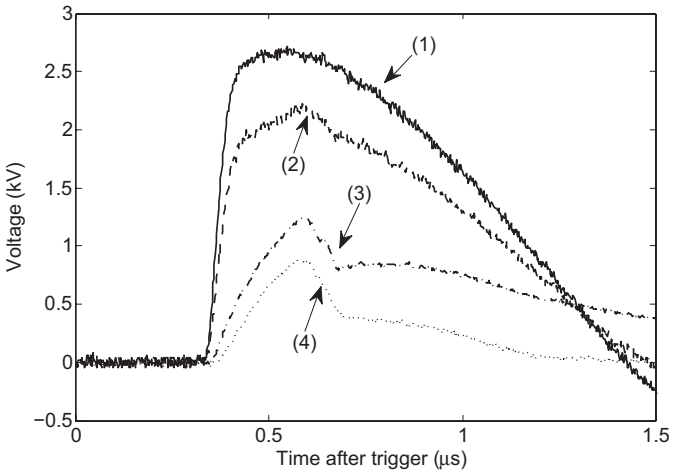

Fig. 6. Voltage waveforms during the first 1.5 μs of a pulse measured at four locations in the circuit. (1) Between the high voltage side of the 0.1-μF capacitor on the circuit board and the IGBT collectors. (2) Across the pulse transformer primary. (3) Across the pulse transformer secondary. (4) Between the ignitron ignitor and cathode. Waveforms (3) and (4) have been divided by 2 to remove the effect of the transformer voltage step-up and facilitate the identification of resistive and inductive voltage drops. The capacitor-to-collector voltage on the circuit board does not reach the full 3-kV charging voltage because of incomplete turn-on of the IGBTs at early times (i.e., the voltage drop across the IGBTs does not immediately fall to zero upon triggering, so at early times the collectors are several hundred volts above board ground).

excellent fit to the data. Referring to (6), the total effective inductance that contributes to the rise time is

$$L_{\text{eff}} \equiv L_1\left(1-\kappa^2\right)+\frac{L_1}{L_2}L_s+L_p \tag{7}$$
$$= 1.50\ \mu\text{H}+\frac{1}{4}\times 0.90\ \mu\text{H}+0.78\ \mu\text{H}=2.51\ \mu\text{H}$$

with the dominant contribution coming from the pulse transformer.

VI. Conclusion

The circuit described here was used successfully to trigger a size A 7703 ignitron for the Caltech spheromak experiment [15], an experiment in which the ignitron impedance dominates over the plasma impedance in determining the overall discharge circuit behavior [1] and fast triggering of the ignitron is critical. Our ignitron driver should be widely applicable for other experiments that use ignitrons for switching on microsecond timescales.

In light of the discussion in Section V, there is some room for improvement in the pulse rise time if the circuit layout were optimized to reduce the load inductance: the circuit board, pulse transformer, and ignitron could be mounted closer together than in our experiment, or the connecting wires could be replaced by coaxial cables. However, the main limiting factor is the pulse transformer. With specialized winding techniques, it should be possible to achieve κ closer to unity than in our transformer and thus reduce the leakage inductance.

It should be noted that the total energy stored in the 0.1-μF capacitor in the circuit presented here is 0.45 J, while ignitron manufacturers typically recommend using a trigger pulse energy of 4–7 J to minimize deterioration of the ignitor over time [5]. For high repetition rate applications in which the overall ignitron lifetime is an important consideration, the capacitance or charging voltage should be increased to comply with this recommendation. In this case, additional modifications to the circuit, such as changing the transformer turns ratio, adding more resistance in series with the ignitor, or adding additional IGBTs may be required to avoid exceeding the maximum voltage and current ratings of the IGBTs and ignitor.

References

[1] D. Kumar, A. L. Moser, and P. M. Bellan, "Energy efficiency analysis of the discharge circuit of the Caltech spheromak experiment," *IEEE Trans. Plasma Sci.*, vol. 2, no. 1, pp. 47–52, Jan. 2010.

[2] R. P. Golingo, U. Shumlak, and B. A. Nelson, "Formation of a sheared flow Z pinch," *Phys. Plasmas*, vol. 12, no. 6, pp. 062505-1–062505-9, Jun. 2005.

[3] F. Paganucci, M. Zuin, M. Agostini, M. Andrenucci, V. Antoni, M. Bagatin, F. Bonomo, R. Cavazzana, P. Franz, L. Marrelli, P. Martin, E. Martines, P. Rossetti, G. Serianni, P. Scarin, M. Signori, and G. Spizzo, "MHD instabilities in magneto-plasma-dynamic thrusters," *Plasma Phys. Control. Fusion*, vol. 50, no. 12, p. 124010, Dec. 2008.
[4] J. M. Taccetti, T. P. Intrator, G. A. Wurden, S. Y. Zhang, R. Aragonez, P. N. Assmus, C. M. Bass, C. Carey, S. A. deVries, W. J. Fienup, I. Furno, S. C. Hsu, M. P. Kozar, M. C. Langer, J. Liang, R. J. Maqueda, R. A. Martinez, P. G. Sanchez, K. F. Schoenberg, K. J. Scott, R. E. Siemon, E. M. Tejero, E. H. Trask, M. Tuszewski, and W. J. Waganaar, "FRX-L: A field-reversed configuration plasma injector for magnetized target fusion," *Rev. Sci. Instrum.*, vol. 74, no. 10, pp. 4314–4323, Oct. 2003.
[5] *National Electronics*, Standard NL7703, Jun. 2009.
[6] J. H. Sondericker, "Shunt triggered flashtube illumination system design," *Rev. Sci. Instrum.*, vol. 37, no. 12, pp. 1705–1707, Dec. 1966.
[7] P. K. Loewenhardt, M. R. Brown, J. Yee, and P. M. Bellan, "Performance characterization of the Caltech compact torus injector," *Rev. Sci. Instrum.*, vol. 66, no. 2, pp. 1050–1055, Feb. 1995.
[8] I. Trabjerg, "Pulsed magnet for magneto-optical experimentation," *Rev. Sci. Instrum.*, vol. 51, no. 10, pp. 1326–1329, Oct. 1980.
[9] G. H. W. Behrendt and N. Gothard, "Inexpensive ignitron discharge circuit," *Rev. Sci. Instrum.*, vol. 39, no. 9, p. 1376, Apr. 1968.
[10] B. B. Pollock, D. H. Froula, P. F. Davis, J. S. Ross, S. Fulkerson, J. Bower, J. Satariano, D. Price, K. Krushelnick, and S. H. Glenzer, "High magnetic field generation for laser-plasma experiments," *Rev. Sci. Instrum.*, vol. 77, no. 11, pp. 114703-1–114703-6, Nov. 2006.
[11] A. Kumar, V. Chaudhari, K. Patel, S. George, S. Sunil, R. K. Singh, and R. Singh, "An experimental setup to study the expansion dynamics of laser blow-off plasma plume in variable transverse magnetic field," *Rev. Sci. Instrum.*, vol. 80, no. 3, pp. 033503-1–033503-6, Mar. 2009.
[12] *Very High Voltage IGBT IXEL40N400*, IXYS Corporation, Santa Clara, CA, USA, Dec. 2009.
[13] *Rectifier Applications Handbook (HB214/D)*, 2 ed., ON Semiconductor, Phoenix, AZ, USA, 2001.
[14] A. D. Pathak, *Application Note AN0002: MOSFET/IGBT Drivers, Theory and Applications*. Santa Clara, CA, USA: IXYS Corporation, 2001.
[15] S. C. Hsu and P. M. Bellan, "Study of magnetic helicity injection via plasma imaging using a high-speed digital camera," *IEEE Trans. Plasma Sci.*, vol. 30, no. 1, pp. 10–11, Feb. 2002.

Vernon H. Chaplin received the B.A. (high Hons.) degree in astrophysics from Swarthmore College, Philadelphia, PA, USA, in 2007. He is currently pursuing the Ph.D. degree in physics with the California Institute of Technology, Pasadena, CA, USA.

His current research interests include laboratory simulations of astrophysical jets and solar coronal loops, spheromak formation, RF plasma sources, pulsed power systems, and plasma spectroscopy.

Paul M. Bellan received the B.Sc. (Hons.) degree from the University of Manitoba, Winnipeg, MB, Canada, in 1970, and the M.A. and Ph.D. degrees in plasma physics from Princeton University, Princeton, NJ, in 1972 and 1975, respectively.

He was a Post-Doctoral Fellow with the Princeton Plasma Physics Laboratory, Princeton. He joined the Faculty of California Institute of Technology, Pasadena, CA, USA, in 1977, where he is currently a Professor of applied physics. He has authored over 100 scientific publications and two books. His current research interests include experimental and theoretical studies of lower hybrid wave propagation in plasmas, drift Alfvén waves, laser-induced fluorescence of plasmas, stochastic ion heating by coherent drift waves, magnetic helicity injection into tokamaks, spheromak injection into tokamaks, RF current drive in tokamaks, stability of arcs, astrophysical jets, and solar coronal loops.

Dr. Bellan is a fellow of the American Physical Society.